Ultrafast Dynamics in Na-Doped Water Clusters and the Solvated Electron†

H. T. Liu, J. P. Müller, N. Zhavoronkov, C. P. Schulz,* and I. V. Hertel‡

Max Born Institute, Max-Born-Strasse 2a, 12489 Berlin, Germany

Received: August 13, 2009; Revised Manuscript Received: October 22, 2009

The lifetimes of the first electronically excited state of $(H_2O)_n\cdots Na$ and $(D_2O)_n\cdots Na$ clusters up to $n = 40$ have been measured by two-color pump−probe spectroscopy (800 and 400 nm) with 35 fs laser pulses. The excited-state lifetime decreases rapidly from 1.2 ps at $n = 2$ to approximately 100 fs at $n \geq 10$. For $(D_2O)_n\cdots Na$, the average lifetime is about 3.6 times longer. The fast energy redistribution is explained by conversion of the electronic excitation into vibrations of the ground state. A simple model based on Fermi's Golden Rule predicts the observed trends but fails to reproduce the observed lifetimes quantitatively. The longer lifetimes for deuterated clusters are discussed in the framework of the famous energy gap law and indicate that the stretching modes of water play an important role in the energy-transfer process.

Introduction

When alkali metal atoms are introduced into a polar liquid, the weakly bound alkali valence electron is separated from its ionic core and dissolved in the liquid. These excess electrons are called "solvated" electrons because it is commonly accepted that they are localized in a void surrounded by the polar solvent molecules.[1–3] The formation dynamics of the solvated electron is of great scientific interest and has been studied in the liquid phase extensively.[4–9] While the different experiments give a common picture of the observed decay times, there is still a controversy about the interpretation of the fairly complicated transient absorption spectra.[10–12]

A complementary approach to investigate the formation and photodynamics of the solvated electron comes from cluster science. Studying finite systems of well-defined sizes enables a fundamental understanding of properties of matter by following their changes from the molecular to the macroscopic scale. In the context of the celebrated solvated electron negatively charged clusters such as $(H_2O)_n^-$ and $(NH_3)_n^-$ serve as model systems.[13–16] Ground-breaking experiments on the dynamics of $(H_2O)_n^-$ clusters have been performed in the Neumark group by using photoelectron imaging and time-resolved photoelectron spectroscopy.[17–19] The Johnson group investigated electronic and vibrational spectra of these clusters.[20–22] The spectroscopy and dynamics of excess electrons in clusters have recently been reviewed in ref 16.

Another model system to study the solvated electron are solvent clusters with an additional alkali atom attached, a method our group has been following for several years. Many different spectroscopic properties of $(H_2O)_n\cdots Na$ and $(NH_3)_n\cdots Na$ clusters have been determined experimentally. After the first observation of $(H_2O)_n\cdots Na$ clusters,[23] the ionization potentials (IP) were determined up to cluster sizes of $n = 20$.[24–26] Buck and co-workers have extended the measurements for $(NH_3)_n\cdots Na$ toward larger sizes.[27] Figure 1 summarizes the results. The ionization potential for both cluster types drops quickly until $n = 4$. For larger clusters, the IP of $(NH_3)_n\cdots Na$ continues to decrease and eventually reaches the bulk work function (WF) for a solvated electron in ammonia at 1.45 eV.[28] The general size dependence of the IP from these clusters was successfully modeled by a simple electrostatic potential using the dielectric properties of the solvents.[25,29] However, for $(H_2O)_n\cdots Na$ clusters having almost the same dielectric properties as ammonia, this model fails to mimic the constant IP for clusters ≥4. The observed constant value of 3.2 eV corresponds to the one which is believed to be the WF of the solvated electron in bulk water.[14] When sodium is replaced by another alkali metal like Li and Cs, the observed IPs for $n \geq 4$ are almost the same.[30,31] The constant IPs for $(H_2O)_n\cdots Na$ ($n \geq 4$) constitutes a challenging puzzle. Several theoretical studies have addressed this problem, but no conclusive answer have been found up to now.[32–35]

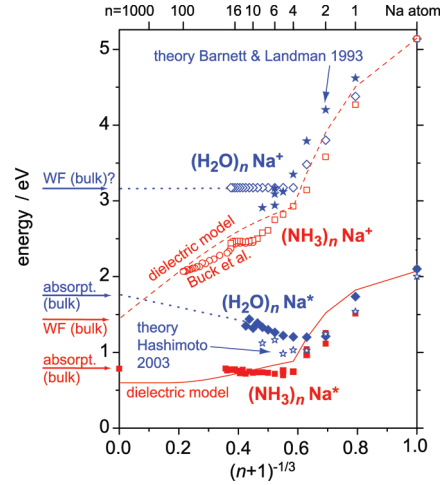

Figure 1. Spectroscopic properties of $(H_2O)_n\cdots Na$ and $(NH_3)_n\cdots Na$ clusters. Ionization potentials and excitation energies from various sources are compared. Diamonds and squares denote data acquired by our group, and IP data from ref 27 are indicated by circles. A dielectric model (dashed line and full line) has been introduced in ref 25. Asterisks represent more sophisticated theories for $(H_2O)_n\cdots Na$ for the vertical IPs[32] and excitation energies.[36] See text for more details.

Figure 1 also shows the energies for the first electronically excited state of $(H_2O)_n\cdots Na$ and $(NH_3)_n\cdots Na$ clusters.[29,36,37] They correspond to the p ← s transition in either the sodium

† Part of the "W. Carl Lineberger Festschrift".

* To whom correspondence should be addressed: E-mail: cps@mbi-berlin.de.

‡ Also part of the Department of Physics, Free University Berlin, Arnimallee 14, 14195 Berlin, Germany.

10.1021/jp907835z
Published on Web 12/01/2009

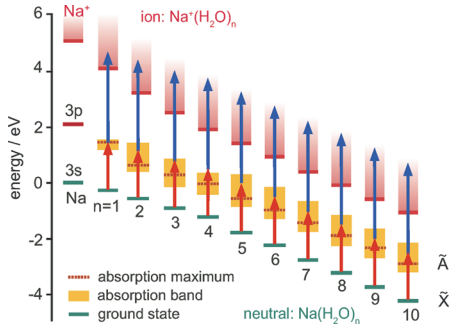

Figure 2. Energy diagram for $(H_2O)_n\cdots Na$ clusters showing the ground, the first electronically excited state, and the ionic continuum of $(H_2O)_n\cdots Na$ clusters.[25,36] The first electronically excited state corresponds to the 3p state of the free sodium atom. The pump pulse at 800 nm and probe pulse at 400 nm are indicated as arrows.

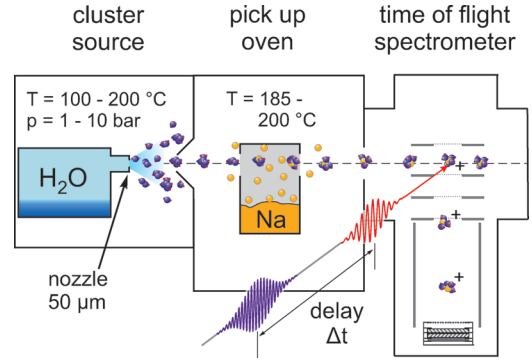

Figure 3. Schematic of the pickup source and the time-of-flight spectrometer. $(H_2O)_n\cdots Na$ clusters are formed in a supersonic expansion of neat H_2O vapor. On their way to the ionization region, they pass through a Na oven to pick up Na atoms.

atom (small cluster limit) or the solvated electron (bulk limit). In the course of these spectroscopic experiments, it was found that the excited clusters may also undergo fragmentation. This raises the question about the nature and time scale of the fragmentation and the associated energy-transfer process.

To address this question, Lineberger and co-workers have studied negatively charged $Cu^-(H_2O)_n$ clusters in a sophisticated femtosecond photodetachment−photoionization experiment.[38,39] This type of experiment interrogates the solvent reorientation dynamics of the neutral ground state after photodetachment. In the case of small $Cu^-(H_2O)_n$ clusters ($n = 1$ and 2), the complex experiences large-amplitude H_2O reorientation and dissociation. No results on larger clusters have been published so far.

The dynamics of the first electronically excited state of $(H_2O)_n\cdots Na$ and $(NH_3)_n\cdots Na$ can be studied by femtosecond two-color pump−probe measurements. Results of the photoinduced dynamics in $(NH_3)_n\cdots Na$ have already been published.[40−42] Similar pump−probe studies on $(H_2O)_n\cdots Na$ clusters are the topic of the present publication. One can expect interesting differences in the exited-state lifetime between the two solvents complementary to the energetic differences observed in the spectroscopic studies. Figure 2 shows the energy levels of $(H_2O)_n\cdots Na$ clusters up to $n = 10$, schematically using all available spectroscopic data.[25,36] The absorption band gets broader with increasing cluster size, as indicated in the figure. Hence, the first excited state of all cluster sizes can conveniently be excited with the fundamental wavelength of a femtosecond Ti:Sapphire laser at 800 nm. For the ionizing step, the second harmonic at 400 nm is sufficient. The energies of the pump and probe photons are indicated as arrows in Figure 2.

The paper is organized as follows. The experimental setup and methods are described in the next section. That section is followed by a presentation of the experimental data and their discussion. A simple model of the excited-state lifetimes based on the density of states will be discussed, and finally, our results will be compared with results found for negatively charged water clusters. At the end, a conclusion will wrap up our findings.

Experimental Section

Figure 3 shows a sketch of the experimental setup. A detailed description can be found in an earlier publication.[43] Briefly, water clusters are created by expanding water vapor through a conical nozzle with a 50 μm diameter into vacuum. The water oven can be heated up to a temperature of 200 °C, which corresponds to a vapor pressure of 10 bar. To avoid clogging, the nozzle is heated separately and kept 10 to 20 °C warmer than the water oven temperature. Approximately 25 mm downstream from the nozzle, the supersonic jet is collimated by a skimmer (0.7 mm diameter). The beam of water cluster traverses to an oven containing sodium. In the oven, water clusters pick up a certain number of sodium atoms. The average number is determined by the sodium vapor pressure. For doping the water clusters with a single sodium atom, the oven is heated to a temperature of about 195 °C, which corresponds to a sodium vapor pressure of 1.5×10^{-4} mbar. After formation, the beam of sodium-doped water clusters proceeds toward the detector chamber. There, the clusters are excited with a femtosecond pump pulse (800 nm) and ionized with a probe pulse (400 nm). Finally, the cluster ions are mass-separated in a time-of-flight mass spectrometer (Wiley−McLaren type) and detected by microchannel plates. The ion signal is discriminated by a constant fraction discriminator and registered using a fast data acquisition card.

The femtosecond laser pulses are generated by a commercial Ti:Sapphire laser system, which provides sub 30 fs pulses at a wavelength of 800 nm (red) and pulse energies up to 0.8 mJ at a repetition rate of 1 kHz. To create the pump and probe pulses, the laser beam is split into two parts. One is used directly as the pump pulse to excite the clusters. The other beam is focused into a BBO crystal (thickness 100 μm) producing the second harmonic at 400 nm (blue) to ionize the excited clusters. The pump and probe pulses are mildly focused with spherical mirrors ($f = 1000$ mm). They enter the interaction region nearly collinear and intersect the cluster beam perpendicularly. To optimize the spatial overlap of the beams, the ion signal measured at a time delay of $\Delta t = 0$ is maximized. The energy of the red pulse is attenuated to 30 μJ to avoid multiphoton processes. The energy of the blue pulse is also 30 μJ without any attenuation after the BBO crystal. The resulting peak intensity is in the range of 10^{11} W/cm^2. Despite the relatively high intensity, the measurement is performed in the single-photon regime due to the broad absorption band and the consequently low oscillator strengths. This is verified by negligible ion signal from a single laser beam (either red or blue) as compared to the signal when both beams interact with the clusters. The pulse duration has been measured directly by frequency-resolved optical gating and found to be 35 fs (FWHM) for the pump and the probe pulse with a nearly Gaussian shape. From this, we calculated the overall width of the cross-correlation to be $w = 30$ fs at $1/e$ intensity, corresponding to a FWHM of $\Delta t_{1/2} = 50$ fs.

The time delay between the pump and probe pulses is controlled by a stepper-motor-driven linear stage, which is inserted into the pump beam and allows for a time resolution of 0.6 fs. The delay stage is controlled by a PC, which also records the mass spectra.

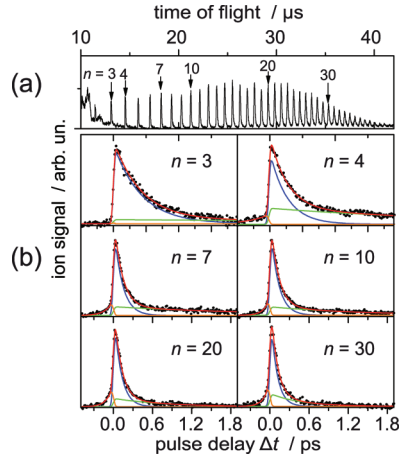

Figure 4. (a) Typical time-of-flight mass spectrum of $(H_2O)_n\cdots Na$ clusters at a pulse delay of $\Delta t = 0$ fs. (b) Integrated ion yields for selected clusters as a function of the pulse delays Δt. The red line denotes the fit function $\Gamma(t)$ according to eq 1. The blue, green, and orange lines presents the different components of the fit function. For details, see the text.

Results and Discussion

For the pump−probe measurements, mass spectra were taken at delay positions with a minimal step size of 5 fs. At each position, ion signals from 10000 to 15000 laser shots were accumulated. Figure 4a shows a typical mass spectrum at zero delay time ($\Delta t = 0$), that is, when the red and the blue pulses overlap in time. One can clearly identify $(H_2O)_n\cdots Na$ mass peaks from $n = 3$ up to 40. The almost symmetric mass peaks indicate that fragmentation does not play a role. Below $n = 3$, the time-of-flight spectrum is distorted by strong ion signals from sodium atoms and dimers emitted directly from the sodium oven as an effusive beam. Thus, we refrain from presenting results for $n = 1$. The result for $n = 2$ has to be taken with some care.

Figure 4b presents the pump−probe signals for some selected $(H_2O)_n\cdots Na$ clusters. For all masses, the ion signal rises sharply at $\Delta t = 0$. Toward positive delay times, where the red pump pulse precedes the blue probe pulse, the ion signal decreases with Δt. In addition, toward negative delay times when the blue pulse acts as the pump while the red one becomes the probe pulse, we also observe a decay with much smaller amplitude. We have found that a convincing fit can be obtained by convoluting the cross correlation $\exp(-\xi^2/w^2)$ of the pulses with three exponential decay functions

$$f(\Delta t) = \int_{-\infty}^{\infty} d\xi \exp(-\xi^2/w^2) \times \{H(\Delta t - \xi)[A \exp((\xi - \Delta t)/\tau) + B \exp((\xi - \Delta t)/\tau_B)] + H(\xi - \Delta t)C \exp((\Delta t - \xi)/\tau_C)\} \quad (1)$$

with $H(x)$ being the Heaviside step function. Typical results are presented in Figure 4b. Zero delay time $\Delta t = 0$ is derived by simultaneously fitting all observed cluster sizes with one free calibration constant. The relaxation times τ and τ_B describe the decay of the ion signal when the red pulse excites and the blue pulse ionizes the $(H_2O)_n\cdots Na$ clusters. The two convoluted exponentials are shown in the figure as blue and green lines, respectively, the dominant feature being the decay with τ, which we attribute to a corresponding loss of population in the electronically excited state. The origin of the weaker signal remains to be discussed. The additional decay with a time constant of τ_C observed toward negative delay times is indicated by the orange line in Figure 4b. We may attribute this signal to the decay of higher-lying electronic states which are excited by the blue pulse and ionized by the red one. The obvious increase of this signal with cluster size supports this assumption since the lower ionization potential for larger clusters increases the density of excited states.[36] The relative magnitude C of this signal contribution is only about 10% of the total signal, and the time constant cannot be determined with sufficient accuracy (it is, however, on the same order of magnitude as that for the first excited state). Thus, we will not further dwell on the interpretation of this signal.

TABLE 1: Excited-State Lifetimes τ for $(H_2O)_n\cdots Na$ Clusters with n Water Molecules

n	τ [fs]	n	τ [fs]	n	τ [fs]	n	τ [fs]
		11	116 ± 15	21	111 ± 10	31	95 ± 25
2	1270 ± 150	12	109 ± 11	22	103 ± 10	32	100 ± 30
3	440 ± 100	13	113 ± 12	23	95 ± 11	33	105 ± 30
4	285 ± 40	14	108 ± 10	24	100 ± 15	34	100 ± 30
5	195 ± 30	15	107 ± 6	25	95 ± 15	35	95 ± 30
6	155 ± 25	16	111 ± 8	26	95 ± 15	36	110 ± 35
7	130 ± 20	17	101 ± 7	27	105 ± 20	37	115 ± 40
8	120 ± 20	18	104 ± 7	28	100 ± 20	38	100 ± 35
9	120 ± 20	19	103 ± 9	29	100 ± 20	39	100 ± 35
10	130 ± 20	20	104 ± 10	30	100 ± 25	40	105 ± 35

The main contribution to the observed ion signal is the exponential decay indicated by the blue line in Figure 4b. This contribution gives the lifetime of the first electronically excited state of $(H_2O)_n\cdots Na$ clusters, which decreases with increasing cluster size. We have been able to determine lifetimes for clusters up to $n = 40$. Table 1 summarizes the data. The values given are mean values over two different experimental runs, which are also used to estimate the errors.

Significant information on the nature of the relaxation mechanism may be expected from a comparison with deuterated

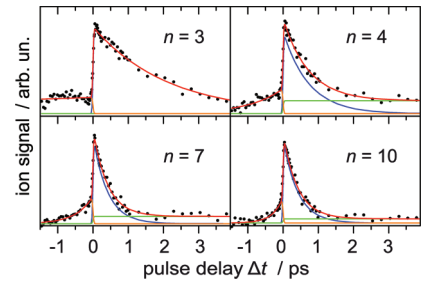

Figure 5. Pump−probe spectra for $(D_2O)_n\cdots$ Na, otherwise identical to Figure 4b.

TABLE 2: Excited-State Lifetimes τ for $(D_2O)_n\cdots$ Na Clusters with n Deuterated Water Molecules

n	τ [fs]	n	τ [fs]	n	τ [fs]
1	$3.1 \times 10^6 \pm 3 \times 10^5$	11	425 ± 35	21	385 ± 40
2	$2.0 \times 10^5 \pm 1.6 \times 10^4$	12	405 ± 45	22	350 ± 50
3	2100 ± 200	13	410 ± 40	23	385 ± 70
4	700 ± 60	14	390 ± 35		
5	610 ± 60	15	385 ± 35		
6	490 ± 40	16	395 ± 40		
7	410 ± 60	17	385 ± 40		
8	415 ± 40	18	410 ± 35		
9	485[a]	19	425 ± 40		
10	420 ± 40	20	380 ± 50		

[a] The ion signal originating from this cluster overlaps with ions from another unknown substance having the same mass (203 u).

clusters, $(D_2O)_n\cdots Na$. Figure 5 shows the experimental data, again together with a fit according to eq 1. Table 2 summarizes the lifetimes for the deuterated clusters up to $n = 23$, also derived from two experimental runs with appropriate errors. As expected, also in this case, the lifetime decreases with increasing cluster size. However, by comparison with Table 1, one immediately notices that the decay times for deuterated clusters are considerably longer than those for $(H_2O)_n\cdots Na$ of the same size. We will come back to this point below.

The general observation is that the lifetime of the first electronically excited state of the $(H_2O)_n\cdots Na$ decreases massively from 1270 fs at $n = 2$ to about 130 fs at $n = 7$. Toward larger cluster sizes, the decrease is much slower and levels off for $n \gtrsim 22$ at about 100 fs. An exception to this trend is the lifetime of $(H_2O)_{10}\cdots Na$, which is distinctly longer than that of the neighboring clusters with $n = 9$ and 11. It is known that the $(H_2O)_n\cdots Na$ clusters have a pronounced solvation shell structure. Theoretical studies[35,36,44] have shown that the first solvation shell is filled after adding four water molecules to the sodium atom. Additional water molecules form a water−water network in the second layer, while the sodium atom remains on the surface of the cluster up to $n = 8$. The 3s valence electron of the sodium atom separates from the ionic core for $n \geq 4$ and forms a delocalized state on the opposite site of the sodium ion, a precursor of the solvated electron. Gao and Liu[35] found in their calculation a change of the structure between $n = 8$ and 10. First, the water molecules start to cover the sodium ion, and second, the distribution of the solvated electron seems to be more localized. These structural changes may lead to the slightly longer decay time for $n = 10$. The measured absorption spectra of $(H_2O)_n\cdots Na$ also show a small jump between $n = 9$ and 10.[36]

It is interesting to compare the decay times of the sodium-doped water clusters with those for the previously studied $(NH_3)_n\cdots Na$ clusters.[42] There, the fast decay times observed have been explained by internal conversion (ic) of the electronic excitation energy into vibrations of the ammonia molecules in the ground state. As the vibrational energy in the cluster increases, the ionization probability decreases due to an unfavorable Franck−Condon overlap with the ionic ground state. Thus, the observed decay times $\tau(n)$ are a direct measure of the electronic to vibrational conversion time. It is fair to assume that the same process occurs in the $(H_2O)_n\cdots Na$ clusters. In the case of sodium-doped ammonia clusters, a simple model calculation based on Fermi's Golden Rule was performed to obtain an estimate of the size dependence for the internal conversion time $\tau(n)$

$$\frac{1}{\tau(n)} = \frac{2\pi}{\hbar}\rho(E,n)|\langle\tilde{A}|W|\tilde{X}\rangle|^2 \qquad (2)$$

with $\rho(E, n)$ denoting the density of states (DOS) of the initially excited electronic state at energy E for cluster size n and $\langle\tilde{A}|W|\tilde{X}\rangle$ the transition matrix element connecting the excited ($\tilde{A}$) with the ground state ($\tilde{X}$) at this internal excitation energy.[42] For a crude estimate, we have assumed here that the transition matrix elements do not depend significantly on the size of the clusters and kept them constant. This can be rationalized by the fact that the excitation energy only weakly depends on the cluster size, which is especially true for larger clusters when the valence electron is separated from the sodium atom ($n \gtrsim 8$). With this approximation, only the DOS as a function of the cluster size has to be determined, which was done by a program using an algorithm from Stein and Rabinovitch.[45]

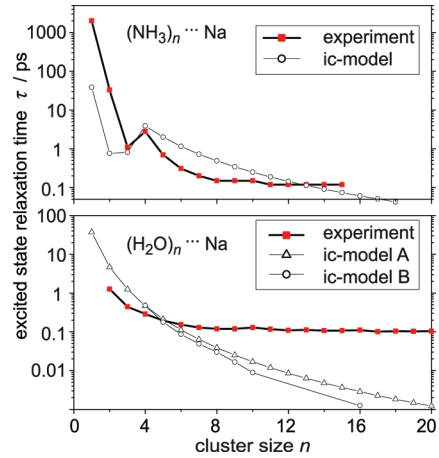

Figure 6. Experimental and calculated excited-state lifetimes versus cluster size. Upper panel: $(NH_3)_n\cdots Na$;[42] lower panel: $(H_2O)_n\cdots Na$.

With this model applied to $(NH_3)_n\cdots Na$ clusters, a reasonably good agreement with the experimentally observed decay times was obtained by only using n times the six internal vibrational modes of the ammonia molecule and ignoring all other intermolecular modes. The result is shown in the upper panel of Figure 6. (The original calculation shown in ref 42 contained a minor error, which has been corrected here.) It can be concluded from this calculation that for sodium-doped ammonia clusters, the internal vibrations are the main accepting modes for energy redistribution.[42]

In Figure 6 (lower panel), the result of the same DOS calculation for $(H_2O)_n\cdots Na$ clusters is shown. In the first calculation (denoted model A), only the $n \times 3$ internal vibrational modes of all water molecules have been used to determine the DOS, that is, the symmetric stretching mode (3657 cm^{-1}), the antisymmetric stretching mode (3756 cm^{-1}), and the bending mode (1595 cm^{-1}). All other intermolecular vibrational modes have been neglected. In contrast to the ammonia case, the calculated conversion times for the $(H_2O)_n\cdots Na$ clusters reproduce the general trend but do not fit the details of our experimental data. With increasing cluster size, the calculated values drop much faster than the experimental ones. In a second calculation (denoted model B), the DOS was determined using the vibrational modes from the calculation given in ref 46, but only the high-frequency modes with energies >1500 cm^{-1}. As shown in Figure 6, in this case, the conversion time drops even faster with increasing cluster size.

For both solvents, the observed decay times show only a very weak size dependence for $n > 8$, while in the DOS calculation, the decay times continuously decrease toward larger clusters. This may indicate that only a limited number of solvent molecules participate in the internal conversion process. Whether or not this signifies that the solvated electron is bound on the surface of the cluster remains to be seen.

The poor agreement of the calculation for small sodium-doped water clusters indicates that the energy redistribution in these excited clusters differs from the one in sodium-doped ammonia clusters. Gao and Liu[35] have performed a quantum chemical calculation where they compare the energetics of these two clusters having different solvents. Especially, they calculated the solute−solvent (ΔE_m) and solvent−solvent (ΔE_s) interaction energies as a function of the cluster size n. Without going into the details of their calculation, the basic results can be summarized as follows. For $(NH_3)_n\cdots Na$ clusters, the interaction of the sodium with the ammonia molecules is always stronger than the interaction between the ammonia molecules. In

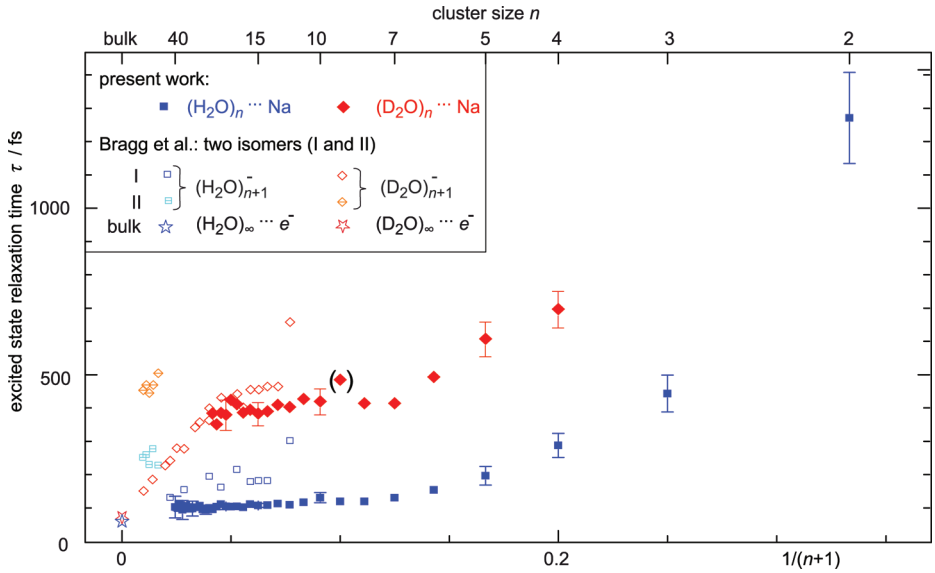

Figure 7. Excited-state lifetimes for $(H_2O)_n\cdots$ Na (blue squares) and $(D_2O)_n\cdots$ Na (red rhombus) as a function of $1/(n+1)$. For comparison, the data for $(H_2O)_n^-$ and $(D_2O)_n^-$ clusters are shown.[19] The lifetimes for bulk water are taken from ref 8.

$(H_2O)_n\cdots$Na clusters, the opposite is true. In these clusters, the strong water−water network determines essentially the structure and thus the energetics. This could be the reason that the simple model calculation is suitable for sodium-doped ammonia clusters but not for the sodium-doped water clusters.

At this point, it is interesting to compare the observed decay times for $(H_2O)_n\cdots$Na and $(D_2O)_n\cdots$Na clusters. The ratio $\tau_D(n)/\tau_H(n)$ as derived from Tables 1 and 2 gives values between 3 and 4 for $n = 3-23$ with an average of $\tau_D(n)/\tau_H(n) \simeq 3.6$. One method to determine the energy-transfer times in a radiationless transition is the famous energy gap law,[47] which reads

$$\tau \propto \exp\left(\frac{\Delta E}{\hbar\omega}\right) \tag{3}$$

ΔE denotes the energy to be transferred (in our case, the excitation energy 1.55 eV = 12500 cm^{-1}), and $\hbar\omega$ is the energy of the accepting vibrational mode, from which follows

$$\tau_D/\tau_H = \exp\left(\frac{\Delta E}{\hbar\omega_D} - \frac{\Delta E}{\hbar\omega_H}\right)$$

independent of the cluster size. The best agreement with the experimental value is obtained when the symmetric stretching mode of water is assumed to be the accepting mode. With 3657 cm^{-1} for H_2O and 2671 cm^{-1} for D_2O, one estimates a value of $\tau_D/\tau_H \simeq 3.5$, while a ratio of 3.2 is obtained when the antisymmetric stretch is assumed to be active (a slightly smaller value but still in the same ballpark). If, however, the bending mode was responsible for the energy transfer, one would obtain $\tau_D/\tau_H \simeq 16$, in strong contrast to the experiment. Thus, it can be concluded that the stretching modes of water play a dominant role in the energy-transfer process.

We already mentioned the relevance of studying Na-doped water clusters for understanding the dynamics of the much-celebrated solvated electron. It is thus challenging to compare the present excited-state lifetimes of sodium-doped clusters with those of water cluster anions intensively studied over the past years in the group of Dan Neumark.[18,19] In our earlier spectroscopic studies, we have already indicated the relation between the ionization potential of the sodium-doped water cluster and the electron affinity of negatively charged pure water clusters.[25] Figure 7 compares the various measured excited-state lifetimes as a function of $1/(n+1)$, with n being the cluster size. The data for water cluster anions have been taken from Bragg et al.[19] The authors distinguish two different isomers denoted as I and II. These two isomers differ in their electron affinity and, as shown in Figure 7, also in their lifetimes. In a first interpretation, it was believed that isomer I has an internally solvated electron, while in isomer II, the solvated electron is localized on the surface of the cluster. After recent calculations by Rossky et al.[48,49] in connection with electronic spectra measured in the Johnson group,[20] a new assignment was proposed; in both isomers, the solvated electron is bound on the surface of the cluster.[16] For up to $n = 24$, this surface state is more localized in isomer I and delocalized in isomer II. Up to now, this controversy was still open.

As seen in Figure 7, the lifetimes of sodium-doped water clusters are significantly shorter than those of water cluster anions for both species, normal and deuterated clusters. Toward larger clusters, this difference becomes smaller. Obviously, the excited-state lifetime is strongly influenced by the structure of the cluster. Especially in small clusters, the structure is dominated by strong sodium(ion)−water bonds. As the size increases, the influence of the direct sodium(ion)−water interaction will be reduced, and the clusters will more and more resemble the structure of water clusters with a solvated electron. In the same way, the vibrational spectra will change as the structure of the cluster changes. In the spirit of eq 2, the excited-state lifetimes are thus correlated to the structure. The almost equal excited-state lifetimes for larger ($n \simeq 30$) water cluster anions and sodium-doped water clusters may be seen as a hint to a similar structure. For a deeper understanding, however, a more quantitative description of the relaxation process is needed, leading our insights beyond the simple model discussed above.

Toward larger clusters with $n > 24$, the excited-state lifetimes of $(H_2O)_n^-$ and $(D_2O)_n^-$ (isomer I) decrease more or less linearly with $1/n$ and appear to eventually reach the bulk values[8] at 50 and 70 fs, respectively. In contrast, isomer II clusters exhibit a longer and nearly size-independent lifetime for sizes with $n =$

60−100, somewhat similar to the second decay with time constant τ_B observed in the present work for the Na-doped water clusters. Recently, Fischer and Dietz have developed a theoretical model for the size dependence of the excited-state lifetimes of solvated electrons.[50] Their model is based on a nonadiabatic long-range coupling mechanism of the solvated electron as a result of dipolar interaction between its p → s transition and the excitation of the infrared-active modes of the solvent water molecules. This model explains the $1/n$ decrease of the excited-state lifetimes observed for isomer I water cluster ions. Unfortunately, with our present experimental setup, we are unable to measure the excited-state lifetimes for sodium-doped water clusters larger than $n \approx 40$. It remains a challenge for the future to determine whether or not sodium-doped water clusters also follow the $1/n$ behavior at larger sizes.

Conclusions

In summary, the lifetimes of the first electronically excited state of $(H_2O)_n\cdots$Na clusters with n up to 40 are determined by two-color pump−probe spectroscopy. The excited-state lifetimes decrease strongly from 1.2 ps for $n = 2$ to 100 fs for $n \geq 10$. The deuterated clusters $(D_2O)_n\cdots$Na exhibit, on average, 3.6 times longer lifetimes. A simple model based on Fermi's Golden Rule failed to quantitatively reproduce the excited-state lifetimes for sodium-doped water clusters, while it was able to describe the lifetimes for $(NH_3)_n\cdots$Na clusters with fairly good agreement. It seems that the tighter water−water network (compared to ammonia) strongly influences the energy redistribution. Nevertheless, the observed ratio of lifetimes from deuterated and nondeuterated clusters indicates that the vibrational stretching modes of water are strongly involved in the process. The exited-state lifetimes for small $(H_2O)_n\cdots$Na clusters are much shorter than those of negatively charged water clusters of the same size. Toward larger clusters, this difference diminishes, indicating that the environment around the excited solvated electron becomes more alike.

To gain a deeper insight into the excited-state dynamics of $(H_2O)_n\cdots$Na clusters, an extension of the experimental data is presently being prepared in our lab using the technique of photoion photoelectron coincidences. From the theoretical point of view, an ab-initio-based model for the photodynamics of water clusters, both alkali-doped and negatively charged, is highly desirable.

Acknowledgment. This work has been supported financially by the Deutsche Forschungsgemeinschaft through SFB 450, Project A2. H.T.L. gratefully acknowledges support by the Alexander von Humboldt foundation.

References and Notes

(1) Jortner, J. *J. Chem. Phys.* **1959**, *30*, 839–846.
(2) Jortner, J. *J. Chem. Phys.* **1961**, *34*, 678–681.
(3) Copeland, D. A.; Kestner, N. R.; Jortner, J. *J. Chem. Phys.* **1970**, *53*, 1189–1216.
(4) Migus, A.; Gauduel, Y.; Martin, J. L.; Antonetti, A. *Phys. Rev. Lett.* **1987**, *58*, 1559–1562.
(5) Long, F. H.; Lu, H.; Eisenthal, K. B. *Phys. Rev. Lett.* **1990**, *64*, 1469–1472.
(6) Kimura, Y.; Alfano, J. C.; Walhout, P. K.; Barbara, P. F. *J. Phys. Chem.* **1994**, *98*, 3450–3458.
(7) Assel, M.; Laenen, R.; Laubereau, A. *J. Phys. Chem. A* **1998**, *102*, 2256–2262.
(8) Pshenichnikov, M. S.; Baltuska, A.; Wiersma, D. A. *Chem. Phys. Lett.* **2004**, *389*, 171–175.
(9) Lindner, J.; Unterreiner, A. N.; Vöhringer, P. *ChemPhysChem* **2006**, *7*, 363–369.
(10) Barnett, R. B.; Landman, U.; Nitzan, A. *J. Chem. Phys.* **1989**, *90*, 4413–4422.
(11) Schwartz, B. J.; Rossky, P. J. *J. Chem. Phys.* **1994**, *101*, 6917–6926.
(12) Scherer, P. O. J.; Fischer, S. F. *Chem. Phys. Lett.* **2006**, *421*, 427–432.
(13) Coe, J. V.; Lee, G. H.; Eaton, J. G.; Arnold, S. T.; Sarkas, H. W.; Bowen, K. H.; Ludewigt, C.; Haberland, H.; Worsnop, D. R. *J. Chem. Phys.* **1990**, *92*, 3980–3982.
(14) Lee, G. H.; Arnold, S. T.; Eaton, J. G.; Sarkas, H. W.; Bowen, K. H.; Ludewigt, C.; Haberland, H. *Z. Phys. D: At., Mol. Clusters* **1991**, *20*, 9–12.
(15) Coe, J. V.; Williams, S. M.; Bowen, K. H. *Int. Rev. Phys. Chem.* **2008**, *27*, 27–51.
(16) Neumark, D. M. *Mol. Phys.* **2008**, *106*, 2183–2197.
(17) Bragg, A. E.; Verlet, J. R. R.; Kammrath, A.; Cheshnovsky, O.; Neumark, D. M. *Science* **2004**, *306*, 669–671.
(18) Verlet, J. R. R.; Bragg, A. E.; Kammrath, A.; Cheshnovsky, O.; Neumark, D. M. *Science* **2005**, *307*, 93–96.
(19) Bragg, A. E.; Verlet, J. R. R.; Kammrath, A.; Cheshnovsky, O.; Neumark, D. M. *J. Am. Chem. Soc.* **2005**, *127*, 15283–15295.
(20) Ayotte, P.; Johnson, M. A. *J. Chem. Phys.* **1997**, *106*, 811–814.
(21) Hammer, N. I.; Shin, J. W.; Headrick, J. M.; Diken, E. G.; Roscioli, J. R.; Weddle, G. H.; Johnson, M. A. *Science* **2004**, *306*, 675–679.
(22) Hammer, N. I.; Roscioli, J. R.; Johnson, M. A.; Myshakin, E. M.; Jordan, K. D. *J. Phys. Chem. A* **2005**, *109*, 11526–11530.
(23) Schulz, C. P.; Haugstätter, R.; Tittes, H. U.; Hertel, I. V. *Phys. Rev. Lett.* **1986**, *57*, 1703–1706.
(24) Schulz, C. P.; Haugstätter, R.; Tittes, H. U.; Hertel, I. V. *Z. Phys. D: At., Mol. Clusters* **1988**, *10*, 279–290.
(25) Hertel, I. V.; Hüglin, C.; Nitsch, C.; Schulz, C. P. *Phys. Rev. Lett.* **1991**, *67*, 1767–1770.
(26) Nitsch, C.; Schulz, C. P.; Gerber, A.; Zimmermann-Edling, W.; Hertel, I. V. *Z. Phys. D: At., Mol. Clusters* **1992**, *22*, 651–658.
(27) Steinbach, C.; Buck, U. *J. Chem. Phys.* **2005**, *122*, 134301.
(28) Häsing, J. *Ann. Phys.* **1940**, *37*, 509–533.
(29) Brockhaus, P.; Hertel, I. V.; Schulz, C. P. *J. Chem. Phys.* **1999**, *110*, 393–402.
(30) Misaizu, F.; Tsukamoto, K.; Sanekata, M.; Fuke, K. *Chem. Phys. Lett.* **1992**, *188*, 241–246.
(31) Takasu, R.; Misaizu, F.; Hashimoto, K.; Fuke, K. *J. Phys. Chem. A* **1997**, *101*, 3078–3087.
(32) Barnett, R. N.; Landman, U. *Phys. Rev. Lett.* **1993**, *70*, 1775–1778.
(33) Hashimoto, K.; Morokuma, K. *J. Am. Chem. Soc.* **1994**, *116*, 11436–11443.
(34) Hashimoto, K.; Kamimoto, T. *J. Am. Chem. Soc.* **1998**, *120*, 3560–3570.
(35) Gao, B.; Liu, Z. F. *J. Chem. Phys.* **2007**, *126*, 084501.
(36) Schulz, C. P.; Bobbert, C.; Shimosato, T.; Daigoku, K.; Miura, N.; Hashimoto, K. *J. Chem. Phys.* **2003**, *119*, 11620–11629.
(37) Nitsch, C.; Hüglin, C.; Hertel, I. V.; Schulz, C. P. *J. Chem. Phys.* **1994**, *101*, 6559–6564.
(38) Muntean, F.; Taylor, M. S.; McCoy, A. B.; Lineberger, W. C. *J. Chem. Phys.* **2004**, *121*, 5676–5687.
(39) Taylor, M. S.; Barbera, J.; Schulz, C. P.; Muntean, F.; McCoy, A. B.; Lineberger, W. C. *J. Chem. Phys.* **2005**, *122*, 054310.
(40) Schulz, C. P.; Höhndorf, J.; Brockhaus, P.; Noack, F.; Hertel, I. V. *Chem. Phys. Lett.* **1995**, *239*, 18–24.
(41) de Vivie-Riedle, R.; Schulz, S.; Höhndorf, J.; Schulz, C. P. *Chem. Phys.* **1997**, *225*, 299–308.
(42) Schulz, C. P.; Scholz, A.; Hertel, I. V. *Isr. J. Chem.* **2004**, *44*, 19–25.
(43) Bobbert, C.; Schulz, C. P. *Eur. Phys. J. D* **2001**, *16*, 95–97.
(44) Hashimoto, K.; Daigoku, K. *Chem. Phys. Lett.* **2009**, *469*, 62–67.
(45) Stein, S. E.; Rabinoviich, B. S. *J. Chem. Phys.* **1973**, *58*, 2438–2445.
(46) Buck, U.; Dauster, I.; Gao, B.; Liu, Z. F. *J. Phys. Chem. A* **2007**, *111*, 12355–12362.
(47) Englman, R.; Jortner, J. *Mol. Phys.* **1970**, *18*, 145–164.
(48) Turi, L.; Sheu, W. S.; Rossky, P. J. *Science* **2005**, *309*, 914–917.
(49) Turi, L.; Madarasz, A.; Rossky, P. J. *J. Chem. Phys.* **2006**, *125*, 014308.
(50) Fischer, S. F.; Dietz, W. *Z. Phys. Chem.* **2007**, *221*, 585–595.

JP907835Z